Applied Chemical Engineering (2024) Volume 7 Issue 1
doi: 10.24294/ace.v7i1.2084

ORIGINAL RESEARCH ARTICLE

Production of Zn-Ti alloy electrodeposition for biomedical applications

Ramesh S. Bhat

Department of Chemistry, NMAM Institute of Technology, NITTE (Deemed to be University), Nitte 574110, Karnataka, India; rameshbhat@nitte.edu.in.

ABSTRACT

Acidic sulphate bath having $ZnSO_4$, $TiSO_4$ and sulphamic acid, was optimized for the deposition of bright Zn-Ti coating on mild steel. The effect of current density, on deposit characters, such as corrosion rate, thickness, and hardness were discussed. Potentiodynamic polarization and electrochemical impedance spectroscopy (EIS) methods were used to evaluate the corrosion properties of the deposit. The composition of deposits was determined by energy dispersive X-ray (EDX) analysis. Scanning electron microscopy (SEM) was used to examine the surface topography of the deposited layer. Atomic force microscopy (AFM) was used to determine the surface roughness. A new and low-priced sulphate bath, for bright Zn-Ti coatings on mild steel has been proposed, and the results indicate better corrosion resistance properties, and these coatings can be used for biomedical tools like Tuning fork, etc, applications.

Keywords: Zn-Ti coating; corrosion; electrodeposition; roughness; SEM

ARTICLE INFO

Received: 30 April 2023
Accepted: 11 July 2023
Available online: 15 December 2023

COPYRIGHT

Copyright © 2023 by author(s). *Applied Chemical Engineering* is published by EnPress Publisher, LLC. This work is licensed under the Creative Commons Attribution-NonCommercial 4.0 International License (CC BY-NC 4.0). https://creativecommons.org/licenses/by-nc/4.0/

1. Introduction

Steel is generally coated with pure zinc to prevent corrosion; however, significant efforts are being made to increase its corrosion resistance for usage in more rasping conditions[1]. Steel is employed in many applications nowadays because of its good corrosion resistance. However, in some industries, including those that use synthetic fibers, waste heat recovery, alternative energy (such as hydrogen production from water electrolysis and proton exchange membrane (PEM) fuel cells), and biomedical applications, steel is vulnerable to corrosion in warm, diluted sulfuric acid. Corrosion strength decreases in acidic media because steel passivation is unstable[2]. Biomaterials are synthetic or natural substances that are directly employed to enhance the functions of living tissue, and they have long been used as implant materials in the field of medicine. Traditional non-biodegradable metallic materials, such as titanium (Ti) and some of its alloys, stainless steels (SS), Ni-Ti, and Co-Cr alloys, are typically employed as permanent or temporary implants to restore function by supporting hard tissues. Because of their excellent mechanical strength and corrosion resistance, these metallic biomaterials have been widely used for a variety of biomedical applications, including joint replacement, fracture fixation, cardiovascular stents, and bone remodeling[3–5].

Hardness, resistance to high temperature oxidation, considerable wear, and corrosion resistance are a few of the many properties of alloy materials. Due to their importance in a variety of fields, the new

alloy materials are being created using a variety of modern procedures. Due to its precise temperature control, rapid deposition rates, and affordability, electrodeposition is one of these technologies that is particularly important for producing alloys. The electrodeposition of Zn-Ni, Zn-Co, Zn-Fe, and Zn-Ni-Co alloys is covered in several scientific articles[6–11]. The structure, morphology, and chemical composition of the Zn-Ni coatings were investigated using XRD and SEM-EDAX techniques, and the corrosion resistance was evaluated using electrochemical experiments[12]. Brenner[13] claims that abnormal Zn-Ni alloy electrodeposition occurs (reduction of less noble zinc is preferred), either as a result of a hydroxide suppression mechanism (release of more noble ions is hampered by the production of $Zn(OH)_2$ to normal pH increase), or both. Recent years have seen a lot of interest in Zn-Ni alloys because they outperform pure Zn and other alloy coatings for Zn-based steel parts in terms of corrosion resistance and mechanical qualities[14]. However, there is an increasing need for Zn-Ni coatings with better mechanical and corrosion properties for industrial applications. Zn-Ni composite coatings have recently been created to satisfy industry standards and enhance mechanical and chemical qualities[15].

Titanium and Zinc may be well known, good antimicrobial, lower the cost of destruction, conserve energy, prevent product contamination, and combat corrosion[16]. The first to conduct an exhaustive examination into the electroplating of alloys and related procedures was Kremann[17]. Materials' physical characteristics, wear resistance, corrosion behaviour, and high-temperature stability of substrates can all be improved through surface modification and specialised treatment for a variety of industrial applications[18–20]. Numerous qualities, including biocompatibility, shape memory, improved wear resistance, and strong corrosion resistance, are present in Ni-Ti coatings. Numerous industries, including biotechnology, electronics, aerospace, automotive, etc., use these alloy coating films[21–25]. Many techniques, including spraying[26], laser ablation[27], magnetron sputtering[28], powder metallurgy[29], and electrodeposition techniques[30–32], have been used to create Ni-Ti alloy films. Among these methods, electroplating is particularly significant since it may be used to create a variety of coatings at room temperature, at a cheap cost, and with a high deposition rate. In the present work, to develop an Zn-Ti alloy coatings on mild steel by electrolytic technique and, their corrosion resistances, microstructure of the deposit and mechanical properties have been discussed and used for biomedical tools like tuning fork etc., applications.

2. Experimental method

We bought a mild steel (MS) substrate from High-Tech Corporation in Mangalore. The fundamental components of mild steel (MS) are 0.063-C, 0.23-Mn, 0.03-S, 0.011-P, and balance-Fe. The MS specimen was collected as a cathode with an exposed surface area of 5.0 cm by 2.0 cm. To achieve the desired finish, the specimen underwent belt grinding, polishing with various emery grades, and velvet mops in accordance with metallographic practice. The specimen was then washed with trichloroethylene, rinsed with distilled water, dried, and utilized for electrodeposition right away[33].

The electrolyte was prepared by using reagent grade chemicals and distilled water. The bath compositions were optimized by trial-and-error method. All coatings at 30 °C and pH of 4.0 were performed, except during their deviation. Plating baths were adjusted to pH 4.0 with dilute solutions of H_2SO_4 and NaOH whenever necessary. The cleaned MS substrate had exposed area of 10 cm^2 was used as a cathode and Zn plate was used as an anode of same area. A 200 mL rectangular poly vinyl chloride cell with a cathode anode distance of ~4 cm has been used. All depositions were galvanostatically performed under the same temperature and pH for 10 min (for assessment) using direct current (DC) power analyzer. Sulphamic acid has been used as complexing agent for the deposition. Based on the surface morphology of the deposit, bath compositions and deposit conditions were optimized.

Electrochemical tests were performed in 5% NaCl solution using a potentiostat (CH604 E-series, U.S. model with CH instrument beta software). Three-electrode cell arrangements were used. A coated MS with a

1 cm^2 exposed area used as the working electrode (WE). A platinum foil with a surface area significantly larger than the WE used as the counter electrode. A saturated calomel electrode (SCE) served as the reference electrode. The corrosion activities of the deposit were studied by PP method and EIS method. By using the PP method and the EIS method, the corrosion activities of the deposit were investigated. The potentiodynamic current-potential graphs were recorded after the specimen was polarised from 200 mV cathodically to +200 mV anodically with respect to OCP at a scan rate of 0.1 mVs1. Corrosion information, including corrosion potential (Ecorr) and corrosion current density (Icorr), were gleaned from the CH instrument's software. In order to analyse the Nyquist plot, the EIS measurements were performed at open circuit potential (OCP) in the frequency range of 100 KHz to 10 MHz.

The throwing power of the plating bath was calculated using the Haring-Blum cell, which is given by the relation 1[34].

$$\text{Throwing power}(\%) = \frac{A - B}{A + B - 2} \times 100 \quad (1)$$

where *B* is the mass ratio of the deposits on near and far cathodes and *A* is the ratio of the distance from far and near cathodes to the anode. The microhardness of the coated films (20 μm) was measured using the Vickers technique at room temperature with a load force of 500 g for 20 s. There were 10 measurements made for every sample. The coating thicknesses were calculated using Faraday's equation:

$$x = (E \times Ic \times A \times \Delta t)/(d \times F) \quad (2)$$

where *x* is the thickness of the film, *E* is its equivalent weight, *Ic* is its current density, *A* is its current efficiency, *t* is the time for the deposit, *d* is its density, and *F* is its Faraday constant (96,500 Coulombs). Analytical scanning electron microscope (JEOL JSM-6380L) at 1000× magnification was used to examine the surface morphology of Zn-Ti coatings. EDX was used to examine the wt.% Ti. Glossmeter (Nova-Elite, 600, ASTM D2457) was used to measure the deposit's reflectivity. The flow chart for the alloy deposition is given in **Figure 1**.

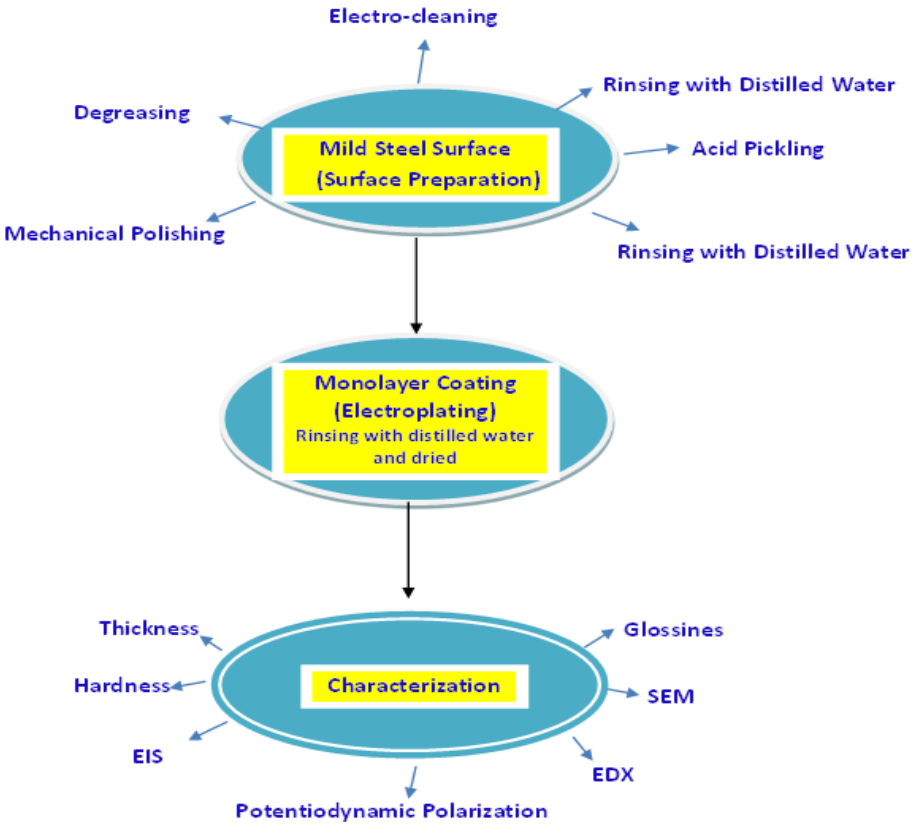

Figure 1. Flow chart for Zn-Ti alloy deposition and characterization.

3. Result and discussion

3.1. Optimization of bath

The acid bath containing $ZnSO_4$ and $TiSO_4$ has been optimized using the conventional Hull cell approach. The deposit characteristics have been found to be significantly impacted by the addition of tiny amounts (1 g/L) of sulphamic acid. The citric acid (CA) was utilized as a buffer to stop the production of hydroxide. To increase the uniformity of the deposit, trisodium acetate was applied as a conducting agent.

It was investigated how each component affected the coatings' morphology, brightness, and appearance. The bath composition and operating conditions for the Zn-Ti alloy bath are shown in **Table 1**.

Table 1. Working conditions and composition of the bath.

Bath constituents	Amount (g/L)
$ZnSO_4$	100
$TiSO_4$	25
$C_6H_8O_7.H_2O$	5.0
$CH_3COONa.3H_2O$	50
H_3NSO_3	1

3.2. Effect of applied current density

3.2.1. Wt.% Ti in the deposit

From optimized baths, wt.% Ti was determined with the effect of applied current densities (ACD). The wt.% of Ti was determined by EDX. It was revealed that ACD plays a significant role in both surface appearance and corrosion performance of the deposit. The change in the appearance and corresponding wt.% Zn and wt.% Ti over a broad spectrum of 1.0–5.0 A/dm^2 is given in **Table 2**. The bath produced white deposit with 0.13 wt.% Ti at low ACD (1 A/dm^2) and a porous bright deposit at high ACD (5 A/dm^2) with 1.80 wt.% Ti A smooth deposit was found at 3.0 A/dm^2 with 1.70 wt.% Ti. It is believed that the quick depletion of more easily deposited Zn^{2+} ions at the cathode coating is caused due to the increase in wt.% of Ti content with current density[35].

3.2.2. Hardness, thickness, glossiness, throwing power of deposit

Hardness, thickness, and glossiness of the Zn-Ti alloy coating was found to increase with current density as shown in **Table 2**. This may be ascribed by the high density of Zn, compared to Ti (d_{Zn} = 7.14 g/cm^3, and Ti = 4.506 g/cm^3). The hardness of the alloy coating with increase in ACD as shown in **Figure 2**. The practical current density was found to show direct dependency on thickness of deposit as given in **Table 2**. The observed linear dependency of the thickness of the coating film with applied current density (ACD) may be due to the adsorbed metal hydroxide at the cathode, caused by the stable increase of pH due to hydrogen evolution at the cathode. The glossiness of Zn-Ti coatings at different current densities were tested and it was found that the deposit formed at low current density showed least glossiness, and at the optimum current density, the glossiness was found maximum. At higher current density, glossiness decreased at higher ACD, due to increased porosity[36].

Table 2. Effect of ACD on hardness, TP, thickness, glossiness, and corrosion rate.

ACD (A/dm^2)	TP (%)	x (µm)	VH_{500}	Glossiness	$-E_{corr}$ (V)	i_{corr} (µA/cm^2)
1.0	15	07.9	123	105	0.710	31.22
2.0	23	09.1	137	121	0.629	26.21
3.0	28	16.3	145	138	0.604	15.29
4.0	25	18.6	151	146	0.649	24.91
5.0	20	21.8	155	159	0.617	28.87

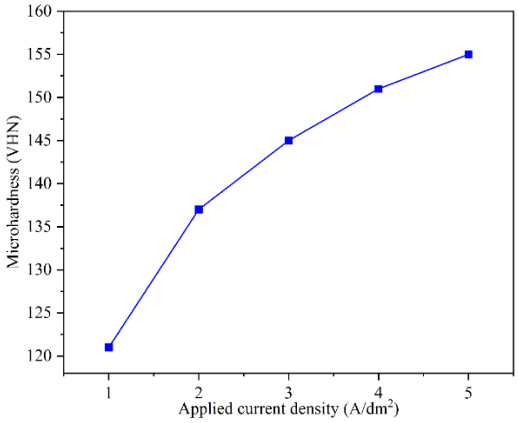

Figure 2. Hardness of Zn-Ti coating film at various ACD.

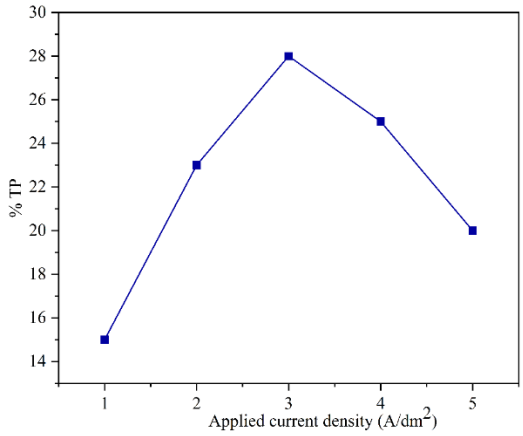

Figure 3. Throwing power of Zn-Ti alloy coating at different ACDs.

Throwing power of the optimized bath at low current density, 1 A/dm^2 was found to be very small 15%. Throwing power was found to be good at 3 A/dm^2 (28%). Further increase in current density 5 A/dm^2, reduces throwing power to 25% at 5 A/dm^2. The throwing power of Zn-Ti alloy coating at different ACDs as shown in **Figure 3**. The glossiness of Zn-Ti alloy coatings at different ACDs was tested and it was found that the deposit shows a minimum glossiness at low ACD, but the glossiness was found to be maximum at the optimum ACD (3 A/dm^2). The glossiness was decreased at high ACD (5 A/dm^2) due to increased porosity[37].

3.3. Corrosion study

Zn-Ti coated samples were subjected to corrosion study in 3.5% NaCl solution and experimental data are given in **Table 2**. The corrosion rate of the alloy coatings was determined by potentiodynamic polarization method. Polarization studies have been made at a scan rate of 0.1 mVs^{-1} in a potential ramp of +0.200V cathodic and −0.200V anodic from open circuit potential (OCP). The calculated E_{corr}, and i_{corr} at different current densities are shown in **Table 2**. The observed results showed that, the coating at 3.0 A/dm^2 shows least corrosion current density i_{corr} = 16.360 µA/dm^2. Potentiodynamic polarization curves for Zn-Ti alloy coating at various ACD as shown in **Figure 4**. This is further supported by its dense, smooth, and uniform surface topography of the coating (**Figure 5b**). Further at higher ACD, increase in Ti content, however, led to an increase in corrosion rate, i.e., due to its thick porous structure of the coating.

3.4. Surface analysis

The surface structure of the deposit at different ACD can be observed from the SEM analysis. **Figure 5a–c** shows the surface topography of Zn-Ti alloy coating at three different ACDs. At low ACD, (1 A/dm^2) the deposit was very thin, light grey, semi bright as shown in **Figure 5a**. At high ACD, (5 A/dm^2) the deposit was thick, porous bright, and large grain size as shown in **Figure 5c** and at optimum ACD, (3 A/dm^2) the deposit

was bright, uniform, and smooth as shown in **Figure 5b**. The wt.% Zn and wt.%Ti at optimum CD = 3A/dm^2 was determined by EDX analysis (**Figure 6**) and the coated sample confirms the presence of Zn (95.99%), Ti (1.70%), and O (2.31%) elements.

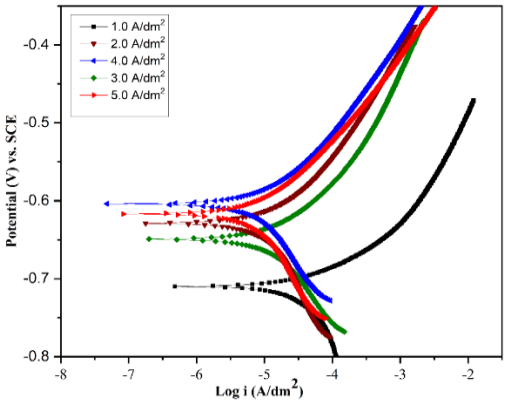

Figure 4. Potentidynamic Polarization curves of Zn-Ti alloy coating at different ACD.

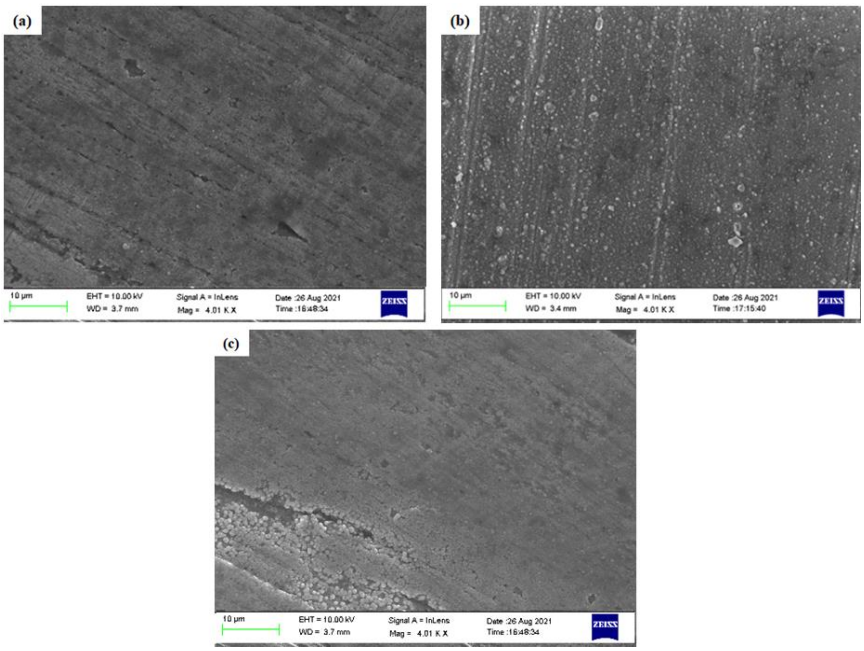

Figure 5. (a–c) Surface morphology of Zn-Ti alloy coating at three different ACD.

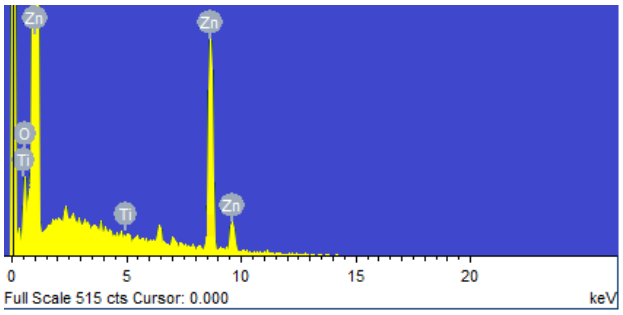

Figure 6. EDX analysis of Zn-Ti alloy film at optimized ACD.

Atomic Force Microscope (AFM), Nanosurf Flex AFM, and Switzerland) were used to compute the mean roughness Ra based on AFM images. **Figure 7** shows the 3D image of Zn-Ti alloy coating at optimized (3A/dm^2) ACD and average roughness (Ra) value is 33.1 nm. Thus, it can be decided that the Zn-Ti alloy film

was less coarse and smooth, homogeneous, and showed small peaks of regular ounce size, resulting in better corrosion resistance (3A/dm^2) and has a lower roughness value as shown in **Figure 7**.

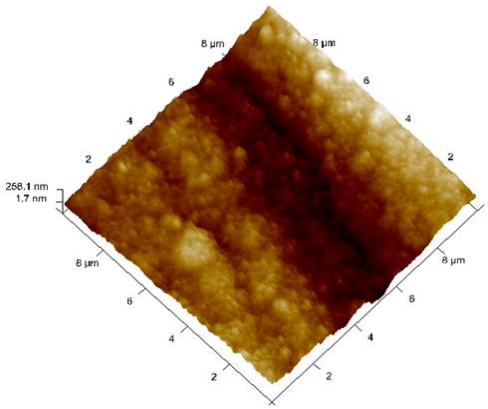

Figure 7. AFM image of Zn-Ti alloy coating (3 A/dm^2).

3.5. EIS analysis

A corrosion measurement technique called electrochemical impedance spectroscopy (EIS) examines the features and dynamics of the electrochemical process at the electrode/solution interface in corrosive solutions. The form of a semicircle is matched by the polarization resistance in Nyquist plots[38,39]. The electrochemical impedance spectroscopy (EIS) is used to pinpoint the electrocatalytic influences on the zinc-Ti alloy coating. The EIS of Zn-Ti alloy coating at different ACD as shown in **Figure 8**.

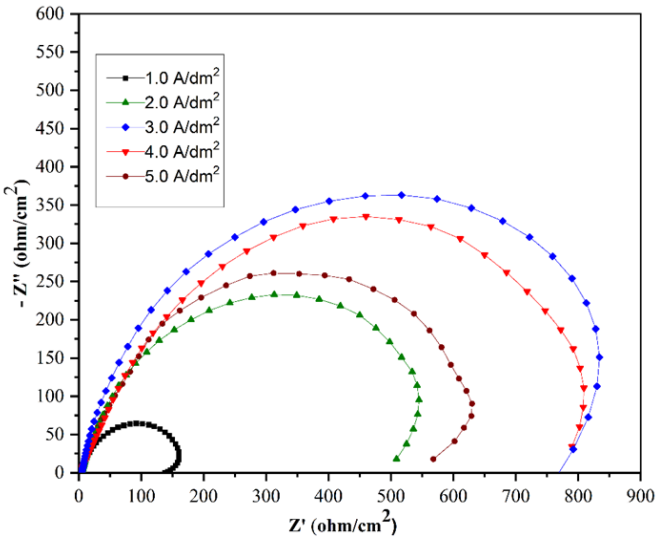

Figure 8. EIS of Zn-Ti alloy coating at different ACD.

It was observed that the radius of the semicircle increases with ACD and decease in semicircle at higher ACD. At low ACD, smaller the semicircle as observed, this may be due thin Zn-Ti coating (**Figure 8**). At higher ACD, decrease in the radius of the semicircle, this may be due to the porosity of the alloy coating, but at optimum ACD radius of the semicircle increases, this may be due to the uniform Zn-Ti alloy coating onto the MS substrate.

4. Conclusion

To produce highly corrosion-resistant Zn-Ti alloy coatings, the process parameters have been optimized. The optimum ACD (3 A/dm^2), the corrosion current density was 15.29 µm/cm^2 and shows highest corrosion resistance. The potentiodynamic polarization and EIS measurements show that Ni and Ti play a key role in the deposit by reducing the rate of corrosion also acts as very good antibacterial activities. The quantity of Zn and

Ti in the coatings directly relates to both the hardness and thickness of the deposits. SEM and AFM examination verified the surface topography and roughness of Zn-Ti coatings, elucidating the reasons for the enhanced corrosion resistance of the coatings. Zn and Ti are showing very good antimicrobial activities, and better corrosion resistance. Therefore, Zn-Ti alloy coatings may have potential uses in the aerospace and biomedical industries.

Conflict of interest

The author declares that no conflict of interest.

Reference

1. Roev VG, Kaidrikov RA, Khakimullin AB. Zinc-Nickel electroplating from Alkaline electrolytes containing Amino compounds. *Russian Journal Electrochemistry* 2001; 37(7): 756–759. doi: 10.1023/A:1016785105516
2. Gahoi A, Wagner S, Bablich A, et al. Contact resistance study of various metal electrodes with CVD graphene. *Solid State Electronics* 2016; 125: 234–239. doi: 10.1016/j.sse.2016.07.008
3. Triclot P. Metal-on-metal: history, state of the art. *International Orthopaedics* 2011; 35(2): 201–206. doi: 10.1007/s00264-010-1180-8
4. Gotman I. Characteristics of metals used in implants. *Journal of Endourology* 1997; 11(6): 383–389. doi: 10.1089/end.1997.11.383
5. Liu Y, Zheng Y, Chen XH, et al. Fundamental theory of biodegradable metals—definition, criteria, and design. *Advanced Functional Materials* 2019; 29(18): 1805402. doi: 10.1002/adfm.201805402
6. Zhang S, Zhang X, Zhao C, et al. Research on an Mg-Zn alloy as a degradable biomaterial. *Acta Biomaterialia.* 2010; 6(2): 626-640. doi.org/10.1016/j.actbio.2009.06.028
7. Gay PA, Berçot P, Pagetti J. Electrodeposition and characterisation of Ag–ZrO_2 electroplated coatings. *Surface and Coatings Technology* 2001; 140(2): 147–154. doi: 10.1016/S0257-8972(01)01043-X
8. Bhat R, Bekal S, Hegde AC. Fabrication of Zn-Ni alloy coatings from Acid Chloride Bath and its corrosion performance. *Analytical and Bioanalytical Electrochemistry* 2018; 10(12): 1562–1573.
9. Bhat RS, Balakrishna MK, Parthasarathy P, Hegde AC. Structural properties of Zn-Fe alloy coatings and their corrosion resistance. *Coatings* 2023; 13(4): 772. doi: 10.3390/coatings13040772
10. Bhat RS**,** Nagaraj P, Priyadarshini S. Zn–Ni compositionally modulated multilayered alloy coatings for improved corrosion resistance. *Surface Engineering* 2020; 37(6): 755–763. doi: 10.1080/02670844.2020.1812479
11. Yao Y, Yao S, Zhang L, Wang H. Electrodeposition, and mechanical and corrosion resistance properties of Ni-W/SiC nanocomposite coatings. *Materials Letters* 2007; 61(1): 67–70. doi.org/10.1016/j.matlet.2006.04.007
12. Blejan D, Bogdana D, Popb M, et al. Structure, morphology and corrosion resistance of Zn-Ni-TiO2 composite coatings. *Optoelectronics and Advanced Materials—Rapid Communications* 2011; 5(1): 25–29.
13. Brenner A. *Electrodeposition of Alloys*, 1st ed. Academic Press; 1963.
14. Abou-Krisha MM. Effect of pH and Current Density on the Electrodeposition of Zn-Ni-Fe Alloys from a Sulfate Bath. *J. Coat. Tech. Res.* 2012; 9: 775–783. doi: 10.1007/s11998-012-9402-1
15. Hanawa T. Titanium-Tissue interface reaction and its control with surface treatment. *Frontiers in Bioengineering and Biotechnology* 2019; 7: 170. doi: 10.3389/fbioe.2019.00170
16. Oliveira NTC, Guastaldi AC, Electrochemical stability, and corrosion resistance of Ti–Mo alloys for biomedical applications. *Acta Biomater* 5(2009): 399–405. doi: 10.1016/j.actbio.2008.07.010
17. Kremann R. The electrolytic representation of bearings from aqueous solutions (German). Vieweg + Teubner Verlag Wiesbaden; 1914.
18. Shahini A, Yazdimamaghani M, Walker K, et al. 3D conductive nanocomposite scaffold for bone tissue engineering. *International Journal of Nanomedicine* 2014; 9: 167–181. doi: 10.2147/IJN.S54668
19. Yazdimamaghani M, Razavi M, Vashaee D, Tayebi L. Microstructural and mechanical study of PCL coated Mg scaffolds. *Surf. Eng* 2014; 30: 920–926. doi: 10.1179/1743294414Y.0000000307
20. Kuru H, Kockar H, Alper M, Karaagac O. Growth of binary Ni-Fe films: Characterisations at low and high potential levels. *Journal of Magnetism and Magnetic Materials* 2015; 377: 59–64. doi: 10.1016/j.jmmm.2014.10.058
21. Elahinia MH, Hashemi M, Tabesh M, Bhaduri SB. Manufacturing and processing of NiTi implants: A review. *Progress in Materials Science* 2012; 57(5): 911–946. doi: 10.1016/j.pmatsci.2011.11.001
22. Toker SM, Canadinc D, Maier HJ, Birer O. Evaluation of passive oxide layer formation–biocompatibility relationship in NiTi shape memory alloys: Geometry and body location dependency. *Materials Science and Engineering C* 2014; 36(1): 118–129. doi: 10.1016/j.msec.2013.11.040
23. Braz Fernandes FM, Mahesh KK, Martins RMS, et al. Simultaneous probing of phase transformations in Ni-Ti thin film shape memory alloy by synchrotron radiation-based X-ray diffraction and electrical resistivity. *Materials Characterization* 2013; 76: 35–38. doi: 10.1016/j.matchar.2012.11.009

24. McMahon RE, Ma J, Verkhoturov SV, et al. A comparative study of the cytotoxicity and corrosion resistance of nickel–titanium and titanium–niobium shape memory alloys. *Acta Biomaterialia* 2012;8(7): 2863–2870. doi: 10.1016/j.actbio.2012.03.034
25. Fadlallah SA, El-Bagoury N, Gad El-Rab SMF, et al. An overview of NiTi shape memory alloy: Corrosion resistance and antibacterial inhibition for dental application. *Journal of Alloys and Compounds* 2014; 583: 455–464. doi: 10.1016/j.jallcom.2013.08.029
26. Tria S, Elkedim O, Hamzaoui R, et al. Deposition and characterization of cold sprayed nanocrystalline NiTi. *Powder Technology* 2011; 210(2): 181. doi: 10.1016/j.powtec.2011.02.026
27. Sharma SK, Mohan S. Effect of chemical treatment on surface characteristics of sputter deposited Ti-rich NiTi shape memory alloy thin-films. *Journal of Alloys and Compounds* 2014; 592: 170–175. doi: 10.1016/j.jallcom.2013.12.266
28. Zeng Q, Xu Y. A comparative study on the tribocorrosion behaviors of AlFeCrNiMo high entropy alloy coatings and 304 stainless steels. *Mater. Today Commun* 2020; 24: 101261.
29. Tosun G, Ozler L, Kaya M, Orhan N. A study on microstructure and porosity of NiTi alloy implants produced by SHS. *Journal of Alloys and Compounds* 2009; 487(1): 605–611. doi: 10.1016/j.jallcom.2009.08.023
30. Kanani N. *Electroplating—Basic Principles, Processes and Practice*. Elsevier; 2006.
31. Bhat R, Bhat UK, Hegde AC. Optimization of deposition conditions for bright Zn-Fe coatings and its characterization. *Prot. Met. Phys. Chem. Surf.* 2011; 47: 645. doi.org/10.1134/S2070205111050030
32. Bhat RS, Shet VB. Development, and characterization of Zn–Ni, Zn–Co and Zn–Ni–Co coatings. *Surface Engineering* 2020; 36: 429–437. doi: 10.1080/02670844.2019.1680037
33. Vogel AI. *Quantitative Inorganic Analysis*. Longmans Green and Co, London; 1951.
34. Bhat RS , Hegde AC. Corrosion Behavior of Electrodeposited Zn-Ni, Zn-Co and Zn-Ni-Co Alloys. *Anal. Bioanal. Electrochem.* 2011; 3(3): 302–315.
35. Bhat RS, Hegde AC. Optimization of bright Zn-Co-Ni alloy coatings and its characterization. *Anal. Bioanal. Electrochem.* 2013; 5(5): 609–621.
36. Bhat RS, Bhat KU, Hegde AC. Layered coating of Zn-Co alloys on mild steel using triangular current pulses for better corrosion protection, *Trans. Indian Inst. Met.* 2013; 66(6): 193–199. doi: 10.1007/s12666-013-0242-1
37. Abou-Krisha MM. Effect of pH and current density on the electrodeposition of Zn–Ni–Fe alloys from a sulfate bath. *Journal of Coatings Technology and Research* 2012; 9(6): 775–783. doi: 10.1007/s11998-012-9402-1
38. Bhat RS. Fabrication of Multi-Layered Zn-Fe alloy coatings for better corrosion performance. In: *Liquid Metals*. *IntechOpen*. 2021.
39. Tozar A, Karahan IH. Structural and corrosion protection properties of electrochemically deposited nano-sized Zn–Ni alloy coatings. *Applied Surface Science* 2014; 318: 15–23. doi: 10.1016/j.apsusc.2013.12.020